

PERIODICO di MINERALOGIA
established in 1930

*An International Journal of
MINERALOGY, CRYSTALLOGRAPHY, GEOCHEMISTRY,
ORE DEPOSITS, PETROLOGY, VOLCANOLOGY
and applied topics on Environment, Archaeometry and Cultural Heritage*

High density silica phases as evidence of small-scale hypervelocity impacts: the Gebel Kamil Crater (Egypt)

Gian Paolo Sighinolfi¹, Chiara Elmi^{1,*}, Romano Serra², and Gabriele Contini¹

¹Dipartimento di Scienze Chimiche e Geologiche, Università di Modena e Reggio Emilia,
Largo S. Eufemia 19, 41121 Modena, Italy

²Dipartimento di Fisica e Astronomia, Università di Bologna, viale Berti Pichat 6/2, 40127 Bologna, Italy

*Corresponding author: chiara.elmi@unimore.it

Abstract

The Kamil Crater is a recent well-preserved impact crater in south-eastern Egypt formed by the explosive hypervelocity impact of a metallic impactor on hypersilic sedimentary rocks. The present study deals with the distribution of high P-T silica phases in different materials present in the crater and in surrounding formations (target rocks, fallback deposits, ejected impact products, and aeolian sands). X-ray diffraction analysis reveals that coesite is ubiquitously present in all materials analyzed, including aeolian sediments collected at considerable distance (> 700 m) from the crater. Impactite clasts exhibit quite variable high P-T silica phase associations. Stishovite occurs exclusively in coesite-bearing impactites accompanied in one sample by mullite. High-T low-P silica polymorphs (cristobalite) were found in some strongly vitreous impactites proximal to the crater. Data suggest that in the case of small-scale hypervelocity impacts occurring in siliceous terrains, high P-T silica phases together micro-deformations in shocked quartz may represent the most suitable diagnostic parameters, especially for old impacts when primary features could be completely hidden by alteration processes.

Key words: high T-P silica phases; coesite; stishovite; Gebel Kamil Crater.

Introduction

After the first discovery of coesite and stishovite by Chao et al. (1961, 1962) in target rocks from the Meteor Crater (Arizona, USA), a

series of occurrences of these phases in terrestrial rocks have been reported, almost exclusively associated with potential impacts of extraterrestrial bodies. Coesite and stishovite are commonly present in a series of materials from

large-scale impact craters such as in Riess Basin (Stähle et al., 2008), in very old (Archaean) structures such as in the Vredefort Dome (Martini, 1991; Spray et al., 1995) and in a small impact crater (e.g., Wabar crater, Prescott et al., 2004), as well.

Occurrences of high density silica phases were recognized also in sediments directly or indirectly connected to impacts as in microtektite-bearing layers (Glass and Wu, 1993) and in the K/Pg boundary layer (previously called Cretaceous-Tertiary boundary layer, Mchone et al., 1989). Recently the unexpected presence of high P-T phases in sediments was considered as diagnostic evidence of an unknown impact event capable of affecting regional climate (Paliwal et al., 2009).

It is well known (for a review cf. French and Koeberl, 2010) that, apart from the occurrence of high P-T phases, a series of diagnostic parameters are used for identifying terrestrial meteorite impact structures. Basically, these parameters include macro shock-deformation features in impact sites (e.g., brecciation and shatter cones, etc.), micro-deformation features in mineral phases (PFs, PDFs, mosaicism, etc.) in target rocks and in impact products and the presence of non-crystalline (vitreous) phases formed during impact thermal metamorphism.

The interpretation of deformation structures, however, may sometimes be controversial. Development of macro-deformation structures due to shock metamorphism is strictly dependent on the rheological properties of substrate rocks. In addition, in the case of very old or old impact structures, macro-deformation effects could be

completely hidden by alteration processes. On the other hand, most impact micro-deformation features in mineral phases may be confused with similar features present in terrestrial rocks and consequent to terrestrial dynamic (metamorphic) processes. In most cases of controversial interpretation of either macro- and micro-deformation features the occurrence of high P-T phases, owing to their relative (even metastable) stability may be decisive for identifying impact events.

Recently, a very young (< 5000 years) and small (45 m diameter) impact crater was discovered in the Gebel Kamil area, south-eastern Egypt. According to recent studies (Folco et al., 2010; Folco and D'Orazio, 2011a; Folco et al., 2011b; D'Orazio et al., 2011) the structure was the result of an explosive hypervelocity impact related to the fall of a metallic impactor. The lithological nature (hypersilicic) of the substrate and the calculated energy of the impact suggest that high P-T silica phases may be formed during the impact.

In the present study the occurrence and distribution of high P-T silica phases in different materials of the Gebel Kamil crater and surrounding formations, were investigated.

Generalities on the Gebel Kamil Crater

The first announcement of the discovery of a small (45 m diameter) well preserved impact crater in south-eastern Egypt was made by Folco et al. (2010). Geophysical data and field observations (Folco and D'Orazio, 2011a) allow the characterization of the target rocks and of the

spatial distribution of metallic meteorite debris and terrestrial ejecta debris. Their asymmetric distribution suggests that the Kamil crater was formed by a moderately oblique impact (Melosh, 1989), perhaps from the north-western quadrant (Folco et al., 2012b). This scenario is consistent with the asymmetry of the slope of the crater, as observed by Folco and D'Orazio (2011a). Further studies (D'Orazio et al., 2011; Folco et al., 2012a) pinpointed that the impactor consisted of an iron meteorite (ungrouped Ni-rich ataxites).

Assemblages of shock deformation features (PFs, PDFs) in quartz grains of some partially vitreous impactite debris suggest shock pressure higher than 20 GPa (Folco et al., 2012b).

Dating of the Kamil event by thermoluminescence (Sighinolfi et al., 2014 in press) indicates a most possible age interval between about 1600-400 BCE.

Information on substrate rocks and impact products

The Kamil crater is found in sedimentary rocks belonging to the Gilf Kebir Formation, a Late Jurassic to Early Cretaceous formation (Klitzsch et al., 1987) constituted by layered sandstones interspersed with minor siltstone layers. Petrographic observations (see also Urbini et al., 2012) indicated that intracrateric target materials mainly consist of pale, coarse to very-coarse, grained quartz arenite with sub-horizontal bedding outcropping on the internal walls of the crater. Smaller amounts of strongly cemented whitish, fine-grained siltstone layers are interbedded with

the coarse-grained arenites, mostly concentrated towards the top of the sequence.

None of the rocks exposed on the crater walls showed evidence of macroscopic shock deformations such as shearing, brecciation, shatter cones, etc.

The base of the crater is partially filled by an arenite breccia lens and by wind-blown sand deposits which cover part of the northern crater wall. Superimposed on the breccia lens, fine-grained whitish fallback laminated deposits, easily distinguished from the wind-blown sands, cover part of the floor of the crater. They are formed by pulverized target materials immediately deposited after impact.

Parts of the target rocks, excavated by the impact, are present as a continuous veneer of ejecta consisting of a mixture of boulders, blocks, and fine-grained debris (Folco and D'Orazio, 2011a; Folco et al., 2011b). Much of the larger terrestrial ejected debris does not show signs of macroscopic deformation features (shearing, brecciation) and of thermal effects due to the impact. Minor components of ejecta consist of a variety of partially or almost totally melted debris, concentrated along the external border of the crater but also present in the less proximal ejecta blanket.

The most common type of ejected impactites are dark (from dark grey to black) coloured clasts, usually dense and containing impactor-derived components (bedrock quartz crystals embedded in shock melt, Folco and D'Orazio, 2011a). Minor amounts of light-coloured or whitish impactite clasts are also present. Most of them are partly covered by black patinas and

contain segregates and veinlets of black material most of which is made up of dark glass. A study of shock micro-deformation features in quartz grains of vitrified impactites (Folco and D'Orazio, 2011a) suggests high (> 20 GPa) shock pressure confirming the hypothesis of a hypervelocity impact.

Recent or present-day pale pink-coloured aeolian sandy deposits cover most of the areas surrounding the crater and, as reported before, the same wind-blown deposits cover part of the northern inner crater wall.

Analyzed material and methods

Investigations for the present paper included the following materials: i) sandstone and siltstone target rocks outcropping on the internal walls of the crater (5 samples labelled TR); ii) fallback deposits present on the floor of the crater (6 samples labelled FB). Samples were collected at different depths (from surface to 120 cm) with the use of a 30 mm diameter steel sampler. Collecting depths are the following: FB-1 (100-120 cm), FB-2 (80-100 cm), FB-3 (60-80 cm), FB-4 (40-60 cm), FB-5 (20-40 cm), and FB-6 (0.20 cm); iii) ejected impactite clasts (10 samples labelled IC). Localization and main macroscopic features (mass, colour) of eight individual clasts are reported in Table 1. Samples IC-9 and IC-10 are composite samples. The IC9 is prepared from 18 individual smaller (< 20 g mass) dark-coloured clasts collected over larger distances in S-E direction from the crater and the IC10 is prepared by combining materials from eight larger (> 20 g mass) dark-coloured debris

collected in areas proximal (maximum distance = 30 m) to the crater; iv) Aeolian sand deposits (4 samples labelled SB). Details on collecting sites and lithology are reported in Table 1. Representative sampling was assured by collecting surface material (max. 3 cm depth) over relatively wide areas of minimum 10 m². For purposes of normalization, only the fraction < 500 μm was selected by in situ sieving. Sample localizations are reported in Table 1. For samples SB-1 and SB-4, two different particle-size fractions (one fraction < 125 μm and the other < 500 μm and > 250 μm) were investigated.

Estimates of the rough sample mineralogy and qualitative observations of micro-deformation features in quartz grains were made by optical microscope. For loose materials (fallback deposit and aeolian sands), observations were made after sample inglobation into a resin matrix.

X-ray powder diffraction (XRPD) technique was used for estimating main mineralogical paragenesis and the presence of high P-T quartz polymorphs. Qualitative X-ray patterns were collected at room temperature using a Philips X'Pert PRO diffractometer equipped with an X'Celerator area detector (CuK α radiation (40 kV, 40 mA), quartz peak as standard, 2θ range 5-70°).

Preliminary tests, attesting the presence of high P-T silica phases in most samples analyzed with the use of conventional XRPD techniques, led us to discard the adoption of time-consuming chemical sample treatments (Chao et al., 1961; Prescott et al., 2004) to concentrate these phases.

To make a blind test and to evaluate potential detection limits for high P-T silica phases using conventional powder diffractometric techniques,

Table 1. Localization and macroscopic features of materials analyzed in the present study. Collection depths for fallback sediments are reported in the text.

Materials	Localization	Macroscopic features (mass, colour, etc.)
Target rocks		
TR-1	S-SW lower internal wall	Pink-coloured medium to coarse grained arenite
TR-2	S-SW lower internal wall	pale pinkly coloured fine-grained arenite
TR-3	S-SW lower internal wall	whitish pale fine-grained arenite
TR-4	S-SW upper internal walls	white-grey siltstone
TR-5	S-SW upper internal walls	white-grey siltstone
Ejecta impactite clasts		
IC-1	10 m SE from external border	61 g, compact, light-coloured with black patinas
IC-2	25 m SW from external to crater	11.3 g, compact, light-coloured with dark veinlets
IC-3	10 m NE, external to crater base	320 g, light-coloured with black veinlets
IC-4	SW lower internal crater walls	125 g, compact, light-coloured with dark veinlets
IC-5	SW upper internal crater walls	126 g, compact dark -coloured
IC-6	40 m SW from the base crater	14.2 g, light-coloured with black patinas
IC-7	45 m SE from base crater	16.7 g, compact, light coloured
IC-8	50 m SW from the base crater	11.5 g, compact, light coloured
IC-9	composite sample from individual clasts collected at > 30 m distance from the crater rim	n. 20 small (> 20 g) dark-coloured clasts
IC-10	composite sample from individual clasts collected at < 30 m distance from the crater	n. 8 larger (> 20 g) dark clasts
Eolic sands		
SB-1	intracrateric present on the NW crater wall (May 2011)	
SB-2	30 m E from the crater base	
SB-3	200 m S-SE from the crater	
SB-4	700 m NW from the crater rim 22° 01' 23''N; 26° 05' 07'' E	

Egyptian desert sands collected at large distance from the Gebel Kamil area were analyzed. Information on the possible detection limits for coesite and stishovite in hypersilicic materials

was obtained by analyzing two high-P silica phase-bearing impactite samples IC-2 and IC-5 diluted at 25 and 15%, respectively with barren desert sands.

Analytical results

Observations at the optical microscope indicate that all analyzed samples of intracraterial exposed target rocks exhibit strong and very diffused micro-deformation features (PFs, PDFs), which contrast with the apparent absence or scarcity of any macroscopic deformation structures (shearing, brecciation, shatter cones). Shocked quartz grains are also relatively diffused in all samples of fallback sediments. As observed also by Folco and D'Orazio (2011a), typology and abundances of shocked quartz grains in partially vitreous impactite clasts varies markedly from clast to clast, ranging from simple but diffused mosaicism to pervasive planar deformation features with multiple sets of PDF. Relatively abundant shocked quartz grains are present in the aeolian sand sample SB-1 collected within the crater. In this case, it cannot be excluded that they derived from contamination by neighbouring fallback deposits. In all other analyzed sand samples few quartz grains with mosaicism and PF-like features are present but all are of questionable interpretation.

Table 2 resumes the results of the XRPD analysis reporting the main mineralogy, in particular on the presence of high P-T silica polymorphs. Powder diffraction patterns on all bulk powders of all intracrateric target rocks, fallback sediments, and aeolian sands analyzed show the ubiquitous presence of coesite (e.g., samples TR-1 and FB-1 on Figure 1a and b, respectively). Neither stishovite nor high T polymorphs of silica (tridimite, cristobalite) were found in any of these materials, thus they should

be considered absent or present in concentrations below the detection limit of the conventional XRPD technique. Ejecta impactite clasts show a variety of different mineral paragenesis regarding high P and T silica polymorphs. Such phases were not found by XRPD, or they may be present in concentrations below the detection limit of conventional X-ray powder diffractometers in most light coloured clasts characterized by extensive vitrification (i.e., samples IC-4, IC-7, and IC-8) and in IC-9 sample, a composite sample representative of dark-coloured clasts of minor mass (< 20 g). Coesite was found alone in sample IC-6, a small light-coloured clast and in sample IC-10, a composite sample representative of dark impactite clasts of major mass (> 30 g). Stishovite was found with coesite in two relatively large clasts collected on the external rim (IC-1) and inside the crater (sample IC-5). It should be noted that in IC-5 stishovite is accompanied also by a high-temperature polymorph of silica, cristobalite, and high P-T alumina polymorphs (mullite) (Figure 2b). Finally, cristobalite is present alone in two light-coloured impactite clasts (samples IC-2 and IC-3) characterized by extensive melting.

Coesite was found to be ubiquitously present in all samples of aeolian sand analysed. In sample SB-4 collected at a relatively long distance (about 700 m) away from the crater and apparently free of shocked quartz grains coesite was found with stishovite.

Blind test on desert aeolian sand, collected at great distant from the Kamil area, confirmed the absence of high P-T silica polymorphs. The XRPD analyses on the impactite samples (IC-1 and IC-5)

Table 2. Main mineralogy and of high P-T silica phases in different materials from the Gebel Kamil crater area.

Materials	Main mineralogy	High P-T silica phases
Target rocks		
TR-1	quartz, kaolinite, albite	coesite
TR-2	quartz, kaolinite, albite	coesite
TR-3	quartz, kaolinite, albite	coesite
TR-4	quartz, kaolinite, albite	coesite
TR-5	quartz, kaolinite, albite	coesite
Intracrateric fall-back deposit		
FB-1	quartz, kaolinite, albite	coesite
FB-2	quartz, kaolinite, albite	coesite
FB-3	quartz, kaolinite, albite	coesite
FB-4	quartz, kaolinite, albite	Not found
FB-5	quartz, kaolinite, albite	coesite
FB-6	quartz, kaolinite, albite	coesite
Ejecta impactite clasts		
IC-1	quartz	coesite, stishovite
IC-2	quartz, albite	crystalite
IC-3	quartz, albite	crystalite
IC-4	mostly vitreous	Not found
IC-5	quartz, mullite, albite	crystalite, coesite, stishovite
IC-6	quartz	coesite
IC-7	mostly vitreous	Not found
IC-8	mostly vitreous	Not found
IC-9	quartz	Not found
IC-10	quartz	coesite
Eolic sands		
SB-1 <500 μm	quartz, albite	coesite
SB-1 <125 μm	quartz, albite	coesite
SB-2	quartz, kaolinite, albite	coesite
SB-3	quartz, kaolinite, albite	coesite
SB-4	quartz, kaolinite, albite	coesite, stishovite

significantly diluted (15 and 25%) with “barren” desert sands evidenced the presence of coesite but not of stishovite. This suggests that the detection

limits for coesite in hypersilicic materials is well below their effective concentrations present in most Kamil considered materials.

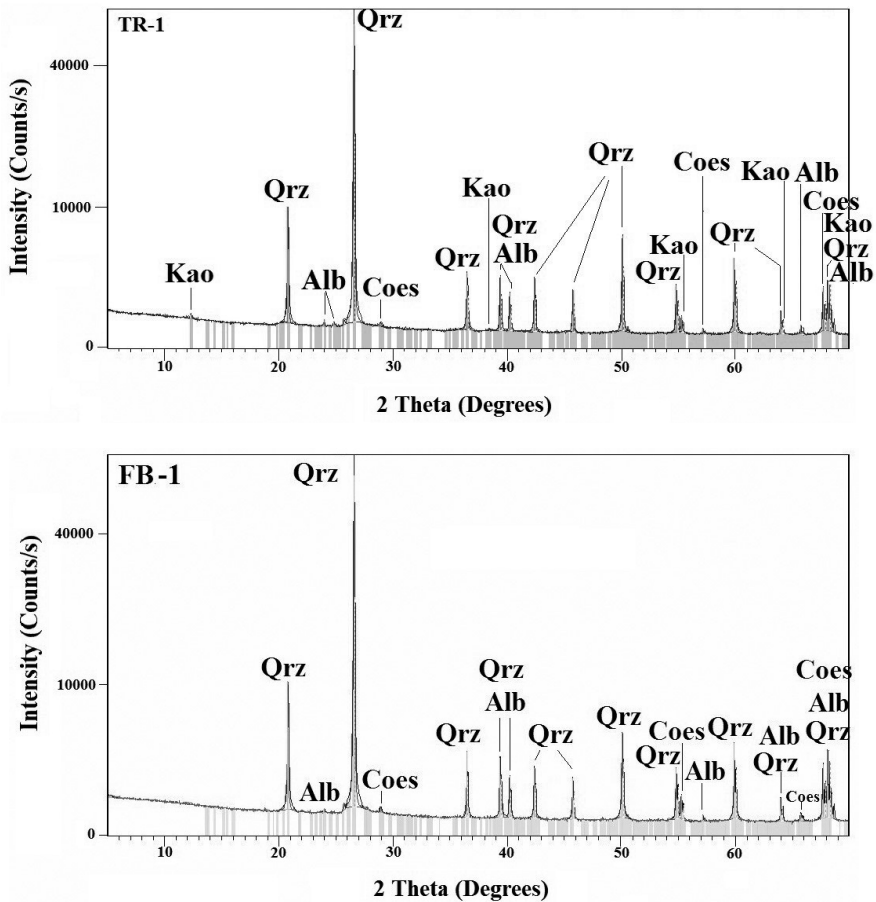


Figure 1. X-ray powder diffraction patterns of sample TR1 (up) and sample FB-1 (below). Kao = kaolinite; Alb = albite; Qrz = quartz; Coes = coesite.

Discussion of the data

Use of diagnostic parameters for small-scale hypervelocity impacts

A wide literature exists on possible parameters, which can be used as diagnostic parameters for terrestrial impacts on different terrains. Most of them, including macro- and

micro-deformations, features were endorsed from studies on major impacts where evidences of the primary structures and impact products are still available. Their relative diagnostic importance may be different in the case of minor impact, where reduced energy and/or impact mode may affect typology of impact products and their dispersion. The comparative analysis of impact different diagnostic parameters in

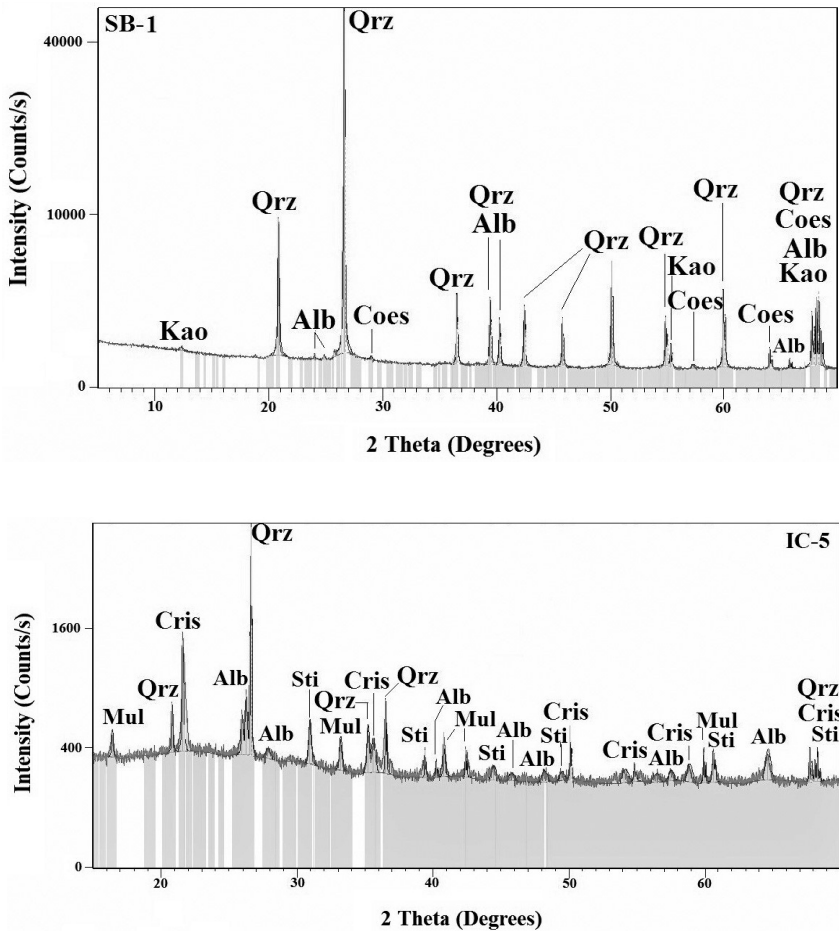


Figure 2. X-ray powder diffraction pattern of sample SB-1 (up) and sample IC-5 (below). Kao = kaolinite; Alb = albite; Mul = mullite; Qrz = quartz; Cris = cristobalite; Coes = coesite; Sti = stishovite.

recent and well preserved structures such as in the Kamil crater can be useful in the choice of most suitable parameters also for the study of old impacts, where surface processes may have destroyed or hidden primary features.

As regards impact macro-deformation features, it is worthy of note the total absence either in the Kamil exposed target rocks and in

proximal and distal ejecta blankets of shatter cones structures, which are usually not destroyed by alteration processes and thus may represent a basic diagnostic parameter in the case of older impacts. In the Kamil structure, clear evidences of macro-deformation features are represented by the intracrateric breccia lenses which provide clear indications that excessive brittle

deformation took place during the cratering event. We did not collect such breccias thus, we cannot assess if they present micro-deformation features able to attribute them to a certain impact origin. Nevertheless, in the case of old small-scale impacts where primary structure may be largely hidden by alteration processes should be problematic to identify such structures based on macro-deformation features. Similar assumption should be made considering micro-deformation features. Findings in Kamil indicate that their presence is restricted in target rocks, perhaps to intracraterial and ejected breccia products and, to minor extent, to products of impact thermal metamorphism. These products are present as ejected partially vitreous clasts and as dispersed micro-particles resulting from melting of both terrestrial and impactor-derived materials (Folco and D’Orazio, 2011a). In the case of the Kamil event, as reasonably in the case of most small-scale hypervelocity impacts, however, the total mass of products of thermal metamorphism is rather limited. In addition, as the products of thermal metamorphism are easily deeply involved in terrestrial alteration processes, in the case of older event, such materials may be not available to be used as impact diagnostic parameter.

Investigations on shock-micro-deformation features in impactite products (Folco and D’Orazio, 2011a) suggest high (> 20 Gpa) shock pressure confirming the hypothesis of a hypervelocity impact. Such conditions may be attained at least part of the target materials originally present in the crater (approximately 3800 m³, according to Urbini et al., 2012). Thus,

taking into account also the hypersilicic nature of the impacted material, we may suggest that a quite large mass of the high-P silica polymorphs were produced by phase transition processes from quartz.

The explosive character of the impact implies that large volumes of both shocked quartz crystals and high-P silica polymorphs are ejected and dispersed over rather large areas around the impact site being deposited on surface surrounding formations. It is well known that the identification of an impact event through the recognitions of shocked mineral grains in loose formations, such as sediments and soils, may be troublesome. Usually, optical observations regarding only reduced amounts of loose material and the interpretation of micro-deformations present in few mineral grains may be sometimes controversial as a series of terrestrial processes which may induce mineral deformations very similar to those of impact shocks.

Diffraction study on the Kamil materials revealed the ubiquitous presence of high-P silica polymorphs (coesite) in all aeolian sediments analyzed. Apart from the sample collected inside the crater perhaps contaminated by materials coming from the crater walls, all aeolian sand samples analyzed are free of quartz grains exhibiting “certain” shock micro-deformation textures. The pervasive presence of coesite in aeolian sediments is rather unexpected. Usually aeolian sands are not locally derived but may result from a transport on longer distances. The data on the Kamil sediments, on the contrary, suggests a relatively low dynamics of aeolian formations after the impact.

Formation of high density phases in the Gebel Kamil event

The lack of information on the mode of occurrence of high P silica phases using adequate analytical techniques (i.e., scanning electron microscope, Raman-laser spectroscopy, etc.) and the reduced number of analyzed samples made it difficult to interpret their genetic processes during the Kamil event. However, their distribution patterns in different materials (target rocks, impactites, loose materials, etc.) and their associations in individual impactite clasts, allowed some hypotheses about their genesis to be considered. Different possible processes of formation of high density phases in impact events were proposed (see e.g., Masaitis, 1998; Feldman et al., 2003, 2007). The most important processes consider recrystallization on solid state stages and crystallization from shock-produced melts (Stähle et al., 2008). Whatever formation process occurs, high density phases usually arise in a very short time (from tenths of a second to seconds) which is defined by the diminishing rate of shock pressure and temperature. Preservation of these minerals depends on the dynamics of temperature changes – they undergo annealing at slow cooling of impactite and consequently more often “survive” in suevite-type and fall out deposits. A process of solid state transition from quartz to coesite is frequently invoked for the presence of coesite in many impact structures (e.g., Kieffer and Simonds, 1980) and it was also experimentally achieved (Kieffer, 1971; Zinn et al., 1997). Experimental data indicated that the solid-state quartz-coesite transition is sluggish under conditions of static

compression while it is accelerated by the presence of shear stresses. It has been seen that in Kamil coesite is the only high-P phase ubiquitously present in exposed target rocks and in their derived fallback deposits obtained by rock pulverization after the cratering event. Taking into account the rheological properties of target rocks and consequently that severe stress conditions must be established during the explosive hypervelocity impact, we could suggest that a solid state martensitic quartz-coesite transition has been the main process responsible for the formation of coesite present in the cited materials.

Much more problematic appears a genetic attribution for the high P and T silica phases present in some partially vitreous impactite ejecta clasts characterized by variable melting degrees as consequence of the impact thermal metamorphism.

Optical observations indicate that high P-T silica phases are usually present only in less vitrified clasts and in clasts of larger mass collected close to the impact site, as IC-5 sample. Sample IC-5 (Figure 2b), collected inside the crater, has a complex XRPD pattern, which shows the coexistence of high P-T silica polymorphs (cristobalite, coesite, and stishovite) and mullite. Mullite was found in other impact structures such as in Popigai crater (Masaitis, 1998; Martinez et al., 1992) and in high-temperature melt products resulting from cosmic airbursts (Bunch et al., 2012). The unique presence of mullite in the IC-5 sample, a relatively large clast affected by low melting and collected inside the crater, seems to be related to

its peculiar terrestrial source and P-T impact evolution history. Chemical data (Authors unpublished data) suggests that this impactite clast, such as other dark-coloured impactites, were not originated from substrate target rocks (i.e., arenites) but from impact shock and thermal metamorphism of materials originally present in a loose alteration sedimentary cover. This latter, which was richer in Al-rich phases such as kaolinite and mullite, may represent the product of P-T metamorphism of such phases. Recently, Kawai et al. (2004) have experimentally observed the high-pressure phase transition of mullite from high-Al phases at pressures above 30.4 ± 3.6 GPa. The occurrence of mullite and high T-P silica polymorphs into the crater suggest high (> 20 Gpa) shock pressure confirming the hypothesis of a hypervelocity impact in Kamil (Folco and D'Orazio, 2011a).

The observed heterogeneity in mineral paragenesis of single Kamil impactite clasts, as similarly found in other larger impact structures, indicates an extreme heterogeneity of physical and chemical conditions, which may determinate non-uniformity of mineral phases development. Studies on impactites of major impacts showed that high-density silica phases are not only associated with diaplectic quartz grains, but are also dispersed in silica amorphous phases (e.g., Stöffler, 1971; Stähle et al., 2008). The lack of information on the mode of occurrence high P-T silica phases by adequate techniques prevents to verify if this similarly occurred also for the Kamil impactites. According to current models and also to experimental data on the shock compression of quartz (Panero et al., 2003),

stishovite would originate from a dense amorphous silica phase producing six-fold coordinated silicon during shock compression under impact loading. Coesite is usually considered (Stöffler et al., 1971) to crystallize behind the shock front, which is, during pressure release, either from a stishovite-like high pressure phase and/or from a silica phase (liquid?) of short-range order with silicon four-fold coordinated. This scenario may be well applicable for the genesis of the coesite and stishovite in some Kamil impactites. The sporadic presence of these mineral phases as well as the presence of cristobalite alone or associated with high- P silica polymorphs in the individual impactite clasts considered in this paper, joins the fact that the metastable persistence of coesite and stishovite is strictly controlled by their individual thermal history.

Acknowledgements

X-ray powder diffraction analyses were carried out at “Centro Interdipartimentale Grandi Strumenti” (CIGS) of Modena and Reggio Emilia University. We are grateful to Luca Bindi and an anonymous reviewer for insightful comments and suggestions.

References

- Bunch T.E., Hermes R.E., Moore A.M.T., Kennett D.J., Weaver J.C., Wittke J.H., DeCarli P.S., Bischoff J.L., Hillman G.C., Howard G.A., Kimbel D.R., Kletetschka G., Lipo C.P., Sakai S., Revay Z., West A., Firestone R.B. and Kennett J.P. (2012) - Very high-temperature impact melt products as evidence for cosmic airbursts and impacts 12,900

- years ago. *Proceeding of the National Academy of Sciences of the United States of America*, E1903-E1912.
- Chao E.C.T., Fahhey J.J., Littler J. and Milton D.J. (1962) - Stishovite, SiO₂, a very high pressure new mineral from Meteor Crater, Arizona. *Journal of Geophysical Research*, 67, 419-422.
- Chao E.C.T., Shoemaker E.M. and Madsen B.M. (1961) - First natural occurrence of coesite. *Science*, 132, 220-222.
- D'Orazio M., Folco L., Zeoli A. and Cordier C. (2011) - Gebel Kamil: The iron meteorite that formed the Kamil crater (Egypt). *Meteoritics & Planetary Science*, 46, 1179-1196.
- Feldman V.I., Sazonova L.V. and Kozlov E.A. (2003) - High density phases as an attribute of impact structures. Conditions of formation and preservation in shock processes (abstract). *Microsymposium*, 38, MS018.
- Feldman V.I., Sazonova L.V. and Kozlov E.A. (2007) - High-pressure polymorph modifications of some minerals in impactites: Geological observations and experimental data. *Petrology*, 15, 224-239.
- Folco L., Di Martino M., El Barkooky A., D'Orazio M., Lethy A., Urbini S., Nicolosi I., Hafez M., Cordier C., van Ginneken M., Zeoli A., Radwan A.M., El Khrepy S., El Gabry M., Gomaa M., Barakat A.A., Serra R. and El Sharkawi M. (2010) - The Kamil crater in Egypt. *Science*, 329, 804.
- Folco L. and D'Orazio M. (2011a) - Shocked quartz at the Kamil crater (Egypt) (abstract). *Meteoritics & Planetary Science Supplement*, 46, A67.
- Folco L., Di Martino M., El Barkooky A., D'Orazio M., Lethy A., Urbini S., Nicolosi I., Hafez M., Cordier C., van Ginneken M., Zeoli A., Radwan A. M., El Khrepy S., El Gabry M., Gomaa M., Barakat A.A., Serra R. and El Sharkawi M. (2011b) - Kamil Crater (Egypt): ground truth for small-scale meteorite impacts on Earth. *Geology*, 39, 179-182.
- Folco L., Fazio A., Cordier C., Van Ginneken M. and D'Orazio M. (2012a) - Microscopic impactor debris in the soil around Kamil crater (Egypt): implications for impact scenario (abstract). *Meteoritics & Panetary Science Supplement*, 47, A132.
- Folco L., Urbini S, Nicolosi I, Zeoli A., El-Barkooky A. and D'Orazio M. (2012b) - Indications of oblique impact directions in terrestrial small-scale impact craters: evidence from Kamil Crater, Egypt. *Meteoritics & Panetary Science Supplement*, 47, A133.
- French B.M. and Koeberl C. (2010) - The convincing identification of terrestrial meteorite impact structures: What works, what doesn't, and why. *Earth-Science Reviews*, 98, 123-170.
- Glass B.P. and Wu J. (1993) - Coesite and shocked quartz discovered in the Australasian and North American microtektite layers. *Geology*, 21, 435-438.
- Kawai N., Nakamura K.G. and Kondo K.-ichi (2004) - High-pressure phase transition of mullite under shock compression. *Journal of Applied Physics*, 96, 4126-4130.
- Kieffer S.W. (1971) - Shock metamorphism of the Coconino Sandstone at Meteor Crater, Arizona. *Journal of Geophysical Research*, 76, 5449-5473.
- Kieffer S.W. and Simonds C.H. (1980) - The role of volatiles and lithology in the impact cratering process. *Reviews of Geophysics*, 18, 143-181.
- Klitzsch E., List F.K. and Pöhlmann G. (1987) - Geological map of Egypt, Gilf Kebir Plateau: Egyptian General Petroleum Corporation/Conoco, 1 sheet, scale 1:500000.
- Martinez I., Guyot F. and Schaerer U. (1992) - Phase transformations in 40-60-GPa shocked gneisses from the Houghton Crater (Canada): An Analytical Transmission Electron Microscopy (ATEM) study. *In Lunar and Planetary Inst., International Conference on Large Meteorite Impacts and Planetary Evolution*, 49-50.
- Martini J.E.J. (1991) - The nature, distribution and genesis of the coesite and stishovite associated with the pseudotachilite on the Vredefort Dome. *Earth and Planetary Science Letters*, 103, 285-300.
- Masaitis V.L. (1998) - Popigai crater: Origin and distribution of diamond-bearing impactites. *Meteoritics & Planetary Science*, 33(2), 349-359.
- Mchone J.F., Nieman R.A., Lewis C.F. and Yates A.M. (1989) - Stishovite at the Cretaceous-Tertiary Boundary, Raton, New Mexico. *Science*, 243, 1182-1184.
- Melosh H.J. (1989) - Impact cratering: A geologic process. Oxford Monographs on Geology and Geophysics 11: Oxford, Oxford University Press, 245 p.
- Paliwal B.S., Shrivastava K.L., Tripathi A., Yadav S.K. and Sisodia H.S. (2009) - X-ray diffraction reveals the presence of mineral coesite and stishovite in the samples of magnetic particles

- collected from the Recent Alluvium of Rajasthan. *Current Science*, 97, 481-483.
- Panero W.R., Benedetti L.R. and Jeanloz R. (2003) - Equation of state of stishovite and interpretation of SiO₂ shock-compression data. *Journal of Geophysical Research*, 108, ECV 5-1-ECV 5-7.
- Prescott J.R., Robertson G.B., Shoemaker C., Shoemaker E.M. and Wynn J. (2004) - Luminescence dating of the Wabar meteorite craters, Saudi Arabia. *Journal of Geophysical Research: Planets*, 109, E01008.
- Sighinolfi G.P., Martini M., Sibilina E. and Contini G. (2014) - Thermoluminescence dating of the Kamil impact crater (Egypt). *Meteoritics & Planetary Science*, In press.
- Spray J.G., Kelley S.P. and Reimold W.U. (1995) - Laser probe argon-40/argon-39 dating of coesite- and stishovite-bearing pseudotachylytic rocks and the age of the Vredefort impact event. *Meteoritics and Planetary Science*, 30, 335-343.
- Stähle V., Altherr R., Koch M. and Nasdala L. (2008) - Shock-induced growth and metastability of stishovite and coesite in lithic clasts from suevite of the Ries impact crater (Germany). *Contributions to Mineralogy and Petrology*, 155, 457-472.
- Stöffler D. (1971) - Coesite and stishovite in shocked crystalline rocks. *Journal of Geophysical Research*, 76, 5474-5488.
- Urbini S., Nicolosi I., Zeoli A., El Khrepy S., Lethy A. and Hafez M. (2012) - Geological and geophysical investigation of Kamil crater, Egypt. *Meteoritics & Planetary Science*, 47, 1842-1868.
- Zinn P., Lauterjung J., Wirth R. and Hinze E. (1997) - Kinetic and microstructural studies of the crystallisation of coesite from quartz at high pressure. *Zeitschrift für Kristallographie - New Crystal Structures*, 212, 691-698.

Submitted, May 2014 - Accepted, August 2014